On diffusion in nanospace

M. Kojic[1,2], M. Milosevic[1], N. Kojic[3], M. Ferrari[2], A. Ziemys[2]

[1]Metropolitan University – Belgrade, R & D Center for Bioengineering, 34000 Kragujevac, Serbia;
[2]The Methodist Hospital Research Institute, Houston, TX 77030;
[3]Tuftts University, Medford, MA 02155;

Abstract

Diffusion in nanospace does not strictly obey to Fick's law generally used in macroenvironment. Deviation from this law is due to surface effects, i.e. due to interaction between transported molecules and bounding surfaces. A hierarchical modeling approach which accounts for interface effects on the diffusion coefficient was introduced in Ziemys et al. (2011). The model employs molecular dynamics (MD) for calculation scaling functions to reduce the diffusion coefficient corresponding to "bulk" values. With this reduced diffusion coefficient, modeling is performed using the finite element method (FE) within an incremental iterative scheme.

In this paper we summarize this hierarchical (multiscale) model and present its generalization to include adsorption at the walls. Also, we briefly discuss further possible applications of the multiscale modeling of diffusion through complex media with distributed solid constituents, as in case of polymers or biological fluids.

Key words: diffusion, molecular transport, molecular dynamics, finite element method, nano-confinement.

1. Introduction

In recent technological fabrication of nanofluidic devices (Grattoni et al. 2010, Gardeniers and Berg 2004) and nanoporous materials (Caro et al 2004, Iijima 1991), transport phenomena within nano-confinement have become very important. The Peclet number of nanofluidic systems ranges from 10^{-6} to 1 with a diffusion coefficient (diffusivity) of 10^{-5} cm^2/s, hence molecular diffusion may dominate the mass transport (Karniadakis 2005).

In common continuum theories of diffusion through homogenous media Fick's law is used as the fundamental relation:

$$J = -D\nabla c \tag{1}$$

where $\boldsymbol{J}$ is the mass flux along concentration gradient ∇c with diffusion coefficient (diffusivity) D. The Stokes-Einstein relation shows that D for an ideal (non-interactive) solution is proportional to molecular mobility μ and thermal energy $k_B T$, or it is inversely proportional to viscosity η and radius r of the diffusing molecule. In real conditions, it is experimentally found

that D depends on concentration, i.e. D=D(c) (English and Dole 1950, Alpert and Banks 1976). However, in nanoconfinement, phase interface may occupy a substantial portion of diffusion domain so that diffusion transport is affected by molecular interactions with the surface, and predictions following Eq. (1) may become inaccurate.

MD modeling and experiments have shown that diffusive transport of molecules and particles in nanochannels is affected by their proximity to a solid surface (Ziemys et al. 2010, Aggarwal et al. 2007). Using MD analysis, it is shown in Ziemys et al. (2010) that molecular diffusivity depends on both concentration and confinement effects. Therefore, modeling of these transport regimes needs novel approaches that could bring molecular scale information into complex macroscale models of nanofluidic devices. MD provides insight into the physics of molecular transport, but it can be used for modeling very small regions, therefore macroscopic methods are necessary. An ideal scenario is to properly transfer MD information to macroscopic models; hierarchical (multiscale) models offer this possibility.

Among various continuum-based numerical methods, which in essence employ a discretization concept, the most developed and well established is the Finite Element Method (FEM). A time and length scale is usually several orders of magnitude larger than in MD. Various schemes have been introduced to couple MD and FEM, as hybrid methods (Rudd and Broughton 1998, Hou and Wu 1997, Broughton et al. 1999), or bridging scale methods (Wagner and Liu 2003, Kojic et al. 2006, 2008a,b).

In this work we present a hierarchical model used to simulate diffusive mass transport in nanofluidic systems, which includes concentration effects and MD derived scaling functions of diffusivity based on proximity to a surface (Arturas et al. 2011). This model is further extended to include adsorption on the wall. Then, we briefly outline possible generalizations to analyze diffusion through complex media, as we have in case of molecular transport within intracellular space or in polymers. Few numerical examples illustrate applicability of our extended hierarchical model. Some concluding remarks are given at the end of this report.

2. Methods

Here, **we** first outline MD simulations, then the FEM, followed by bridging MD-FEM, and finally a concept of including adsorption.

2.1 MD simulations

Molecular Dynamics (MD) has been used for several decades (Rapaport 2004). It is based on statistical mechanics, where motion of particles is described according to the Newtonian mechanics:

$$m_i \dot{\mathbf{v}}_i = \mathbf{F}_i \tag{2}$$

where m_i, $\dot{\mathbf{v}}_i$ and $\mathbf{F}_i$ are mass, acceleration and resulting force (including interaction forces from the neighboring particles and external forces), respectively. The interaction forces include bonded (repulsive-attractive, bending and torsional) and non-bonded (electrostatic, van der Waals) terms. The Force Field (FF) represents a functional form of behavior of chemical structures and is evaluated from potential energy function, $E = E_{intra} + E_{inter}$, of CHARMM FF (MacKerell et al. 1998) used in our MD models:

$$E_{intra} = \sum_{bonds} K_b \left(b - b_0\right)^2 + \sum_{angles} K_\theta \left(\theta - \theta_0\right)^2 + \sum_{torsions} K_\phi \left(1 + \cos\left(n\phi + \delta\right)\right) \tag{3}$$

$$E_{inter} = \sum_{electrostatics} \frac{q_i q_j}{r_{ij}} + \sum_{VDW} \varepsilon_{ij} \left[\left(\frac{R_{min,ij}}{r_{ij}}\right)^{12} + 2\left(\frac{R_{min,ij}}{r_{ij}}\right)^{6}\right] \tag{4}$$

Material parameters of the intramolecular potential E_{intra} are given by the force constants K_b, K_θ and K_ϕ, equilibrium values of bonds and angles b_0 and θ_0, and equilibrium torsions constants – dihedral multiplicity n and dihedral phase δ. Intermolecular potential sums are electrostatic and van der Waals (VDW) terms, where ε_{ij} is VDW potential depth, R_{min} is atom radius, and q_i, q_j are partial atomic charge. These parameters of FF are introduced to represent certain chemical classes of compounds in order to reproduce experimental physico-chemical properties.

MD simulations for calculating diffusivities in nanochannels were carried out (Ziemys et al. 2009, 2010) using NAMD 2.6 (Phillips et al. 2005) with a TIP3P water model (Jorgensen et al. 1983) and NVT (fixed number of particles N, pressure P, volume V) ensembles. CHARMM compatible amorphous silica force field (Cruz-Chu et al. 2006) was employed to model the silica nanochannel, which is modeled by charged hydrophilic amorphous silica phase to match the silica properties after the fabrication process. Glucose diffusion coefficients were calculated from 30 ns trajectories by using the mean square displacement $<r^2>$:

$$<r2>=2dDt \tag{5}$$

where the factor $d = 1, 2, 3$ depends on the dimensionality of the space, and t is time. The diffusivity along the surface normal (z-direction) was evaluated, from the surface up to the middle of the nanochannel. The time window t for $<r^2>$ was chosen as 20 ps, which is small enough to catch local displacements within 0.5 nm thick slabs. The diffusivity results include dependence on distance from the wall and glucose concentrations (Fig 1 – left panel).

The MD calculated diffusivity is normalized with respect to the "bulk" value D_{bulk} corresponding to diffusivity far from the surface, where influence of the surface is negligible. Hence, we have

$$D = SD_{bulk} \tag{6}$$

where

$$S = S\left(w, c\right), 0 \leq S \leq 1 \tag{7}$$

is the scaling function which depends on the distance from the wall surface w and concentration c. Calculated scaling function is shown in Fig. 1 – right panel.
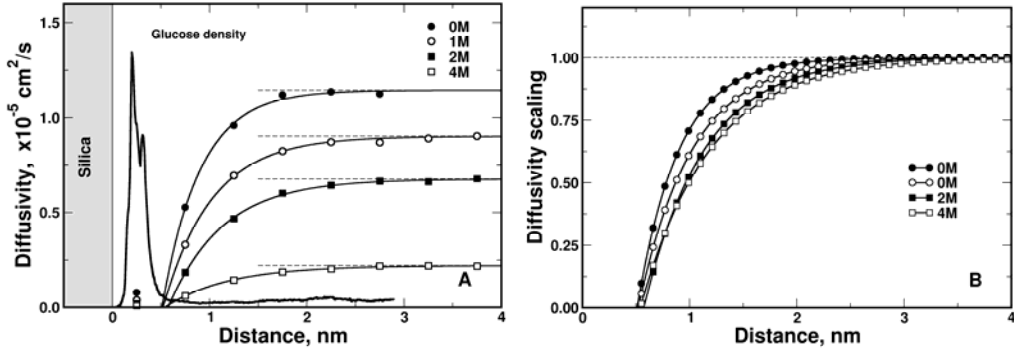
Fig. 1. Calculated glucose diffusivity (left panel)) and scaling functions of the proximity to the silica surface for several concentrations (right panel); according to Ziemys et al. (2011).

Experimental investigations showed that $D(\equiv D_{bulk})$ for glucose depends on concentration, although data are quite different (see Zimys et al. 2011 and references given therein). For examples shown here we have chosen the glucose D according to the largest data set of Gladden and Dole (1953) (Table 1) that spans over a wide range of concentrations, from 0 to 3.36 M.

c,M	$D \cdot 10^{-6}$, cm^2/s
0.00	6.75
0.55	5.80
1.09	4.86
1.66	3.96
2.23	3.02
2.78	2.20
3.36	1.33

Table 1. Experimental data of the diffusion coefficients (Gladden and Dole 1953).

2.2 Finite element model

Finite element modeling of various problems in science and engineering has been well established. We here consider unsteady diffusion where the diffusion coefficient depends on both concentration and spatial position of a point within the model. FE solution procedures for nonlinear diffusion problems have been well established and successfully used in various applications (e.g. Bathe 1996, Hughes 2000, Kojic et al. 2006, 2008a). The basic mass balance equation, which also includes Fick's law in equation (1), is:

$$-\frac{\partial c}{\partial t} + \frac{\partial}{\partial x_i}\left(D\frac{\partial c}{\partial x_i}\right) + q = 0$$

(8)

where $c(x_i,t)$ is concentration; D depends in general on the coordinates x_i and on c; $q(x_i,t)$ is a source term; and summation over the repeated index is implied (i=1,2,3). By using a standard Galerkin procedure, this nonlinear differential equation can be transformed into the incremental-iterative system of linear balance equations for a finite element (Kojic et al. 2008):

$$\left(\frac{1}{\Delta t}\mathbf{M} + {}^{n+1}\mathbf{K}^{(i-1)}\right)\Delta\mathbf{C}^{(i)} = {}^{n+1}\mathbf{Q}^{S(i-1)} + {}^{n+1}\mathbf{Q}^{V(i)} - {}^{n+1}\mathbf{K}^{(i-1)\,n+1}\mathbf{C}^{(i-1)} -$$

$$\frac{1}{\Delta t}\mathbf{M}\left({}^{n+1}\mathbf{C}^{(i-1)} - {}^{n}\mathbf{C}\right) \tag{9}$$

where $\mathbf{C}$ is the vector of nodal concentrations; the left upper indices n and $n+1$ denote values at the start and end of the time step n of size Δt; the indices i and i-1 correspond to the current and previous equilibrium iteration; $\mathbf{Q}^S$ and $\mathbf{Q}^V$ are surface and volumetric nodal fluxes for the element; and components of the matrices $\mathbf{M}$ and $\mathbf{K}$ are:

$$M_{IJ} = \int_V N_I N_J dV \tag{10}$$

$${}^{n+1}K_{IJ}^{(i-1)} = \int_V {}^{n+1}D^{(i-1)} N_{I,i} N_{J,i} dV \tag{11}$$

Here N_I and N_J are the interpolation functions, and ${}^{n+1}D^{(i-1)}$ is the diffusion coefficient corresponding to the last known concentration ${}^{n+1}c^{(i-1)}$ at a point within the finite element. Assembly of equations (9) and solution procedures are performed in a usual manner that is well described in the computational mechanics literature (e.g. Bathe 1996).

In our models we have incorporated concentration and interface effects, according to equation (6) into the FEM model. Implementation of the expression (6) is illustrated in Fig. 2. Note that linear interpolation between scaling curves is used.
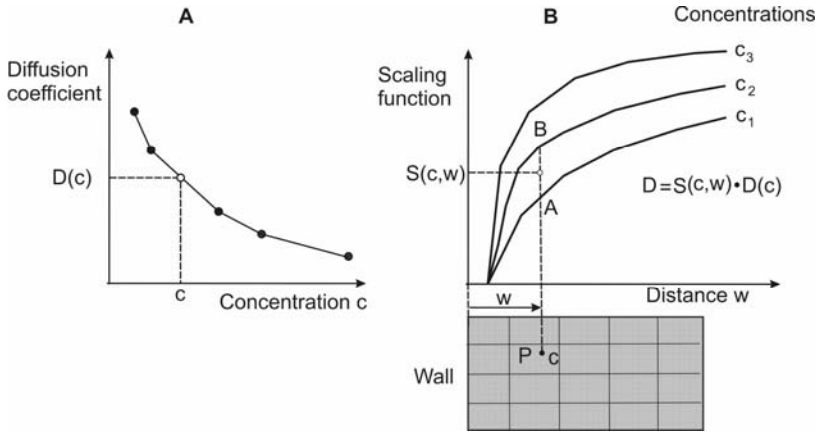
Fig. 2. Determination of diffusion coefficient at a spatial point P using dependence on concentration and surface effects. The "bulk" value is first determined from the curve $D(c)$, A; then the scaling function is evaluated from family of curves shown in B. Linear interpolation curves $S(c,w)$ is adopted (between points A and B in the figure).

The described hierarchical model has been verified by comparison of diffusion experiments in nanochannels (Fine et al. 2010). Good agreement between computed and experimental results for mass release was found (Ziemys et al. 2011).

2.3 FE model with adsorption

The process of adsorption, i.e. attachment of molecules to the surface wall, is an important process occurring in transport of molecules within a nanoconfinement. Here we extend our hierarchical (multiscale) model to include adsorption to the surface. Schematics of the adsorption is shown in Fig. 3.
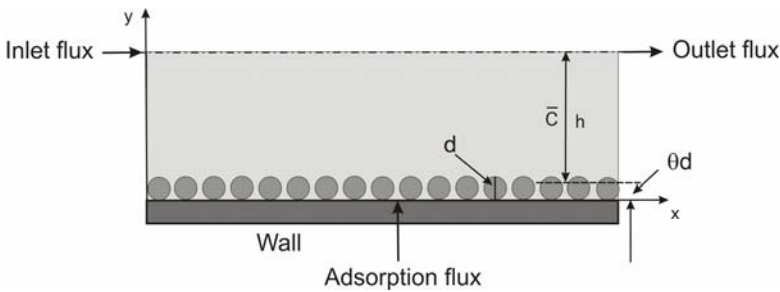
Fig. 3. Schematics of adsorption. Molecules are adsorbed to the wall over time with adsorption flux dependent on the current mean value $\overline{C}$ of concentration along the surface normal and height h. The height of adsorbed layer is θd, where θ is relative area covered by molecules.

The relative area covered by molecules θ is defined as:

$$\theta = \frac{A_{molec}}{A_{total}} \qquad (12)$$

where A_{molec} is area covered by particles (molecules) and A_{total} is the total area. Value θ can be expressed as:

$$\theta = \frac{A_{molec}}{A_{total}} = \frac{k\overline{C}}{1 + k\overline{C}} \tag{13}$$

where $\overline{C}$ is the mean concentration along the surface normal (at a considered point on the surface) and at the height $h = H - \theta d$; and k is the adsorption coefficient.

In the incremental-iterative balance equations (9) must be included adsorption fluxes at the wall, as external fluxes at the FE nodes on the wall boundary. The adsorption flux, which has direction of normal to the wall, can be obtained as follows. Number of molecules $\Delta N(molecules)$ adsorbed at the unit area (1 μ^2)of the wall surface during time step of size Δt is:

$$\frac{\Delta N\left(molecules\right)}{\mu^2} = j_N \Delta t = D \frac{\partial C}{\partial y} \Delta t \frac{N_A}{10^{15}} = D\Delta t\overline{N}_A \frac{\partial C}{\partial y}\left[\frac{molecules}{\mu^2}\right] \tag{14}$$

where j_N is flux in direction of the normal, $N_A = 6.022 \times 10^{23}$ is the Avogadro number, and $\overline{N}_A = 10^{-15}N_A$. Increment of covered area per unit area further is:

$$\Delta\theta\left[\frac{\mu^2}{\mu^2}\right] = D\Delta t\overline{N}_A \frac{d^2\pi}{4} \frac{\partial C}{\partial y} = B_m D\Delta t \frac{\partial C}{\partial y} \quad \left[\frac{\mu^2}{\mu^2}\right] \tag{15}$$

where

$$B_m = \overline{N}_A \frac{d^2\pi}{4} \quad \left[\frac{\mu^2}{Mol}\right] \tag{16}$$

From (15) and (13) follows:

$$Q_y = -\frac{1}{\Delta t B_m}\left(\frac{k^{n+t}\overline{C}}{1 + k^{n+1}\overline{\overline{C}}} - \frac{k^{n}\overline{C}}{1 + k^{n}\overline{C}}\right) \quad \left[\frac{Mol}{\mu^2 s}\right] \tag{17}$$

This final expression is included into equation is included into equation (6) and implemented in the FE program PAK (Kojic et al. 1998, 2009).

2.4 Generalization of the hierarchical model to porous media

Finally, here we outline possible generalization of the hierarchical model to diffusion in complex porous media, consisting of distributed solid constituents within fluid. For simplicity of presentation of this generalization, we assume a medium with solid fibers, as sketched in Fig. 4.
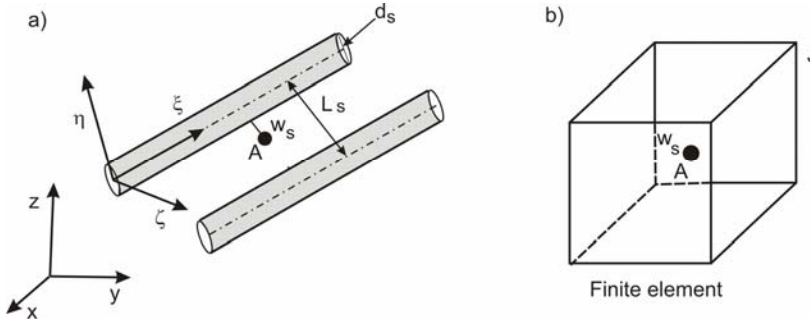
Fig. 4. Concept of extension of hierarchical model to porous medium with fibers. a) Geometry of the internal structure – fibers of a s-group, with diameter d_s and with mutual distance L_s, and point A at distance w_s from the fiber surface; b) Finite element with point A and FE node J.

For a point A in the medium it is possible to calculate the distance from the closest fiber surface of an s-group, and to evaluate scaling function S_s as described above for diffusion within a nanochannel. We assume that scaling functions are different for the normal and tangential directions, hence we have three scaling functions S_ξ^s, S_η^s, S_ς^s in the local fiber directions ξ, η, ξ, so that the diagonal diffusion matrix (tensor) $D_{\xi\xi}^s, D_{\eta\eta}^s, D_{\varsigma\varsigma}^s$ in the local coordinate system is:

$$D_{\xi\xi}^s = S_\xi^s D_0$$
$$D_{\eta\eta}^s = S_\eta^s D_0 \quad\quad\quad (18)$$
$$D_{\varsigma\varsigma}^s = S_\varsigma^s D_0$$

where D_0 is the bulk modulus. The diffusion tensor in the global coordinate system x,y,z can be obtained by tensorial transformation of the second-order tensor,

$$\mathbf{D}_{xyz}^s = \mathbf{T}^s \mathbf{D}_{\xi\eta\varsigma}^s \mathbf{T}^{sT} \quad\quad\quad (19)$$

where the components of the transformation matrix contains cosines of angles between local and global axes:

$$T_{ij}^s = \cos(x_i, \xi_j) \quad i,j=1,2,3 \quad\quad\quad (20)$$

Here x_i and ξ_j stand for global $(x,y.z)$ and local coordinate (ξ, η, ς) systems.

3. Examples

3.1 General description

We use axial-symmetric model of nanochannel (model without reservoirs). According to axial-symmetry concept we are just modeling 2D radial plane with axial-symmetric conditions (axi-symmetric finite elements). Upstream and downstream reservoirs are with 7.85e-009 μl volume each, and at time zero the upstream reservoir was filled with 2.75 M solution, while the other

reservoir had zero concentration. Molar mass of solution is Amol = 100 g/mol, so it can be calculated that initial mass in upstream reservoir is 2.17 e+3 [fg]. Concentration in both reservoirs at the end of FE simulation when the system reaches stationary state will be 1.37 M.

We modeled three different configurations of nanochannels, and all are taken to be with or without adsorption effects. First example is cylindrical model of nanochannel, while other two examples are cones with shrinks at both inlet and outlet cross-sections. Length of cylindrical nanochannel is 50 nm, and radius is 8nm. For conical models we used the same conditions, with the outlet diameter smaller for 8 nm. For FE mesh we used 300 elements in longitudinal direction and 16 elements in radial direction. For each model (with or without adsorption) we present field of concentration and unit mass flux at specific time points of simulation (Figs 5, 6, 9, 10, 11 and 12). For cylindrical model and conical model with shrink at the outlet cross-section we show: diagrams of concentration and Cumulative Mass Release change for both inlet and outlet cross-sections (Figs. 7 and 8); and also diagrams of Relative covered area and Unit Mass Flux-y, according to adsorption effects (Figs 13 and 14).
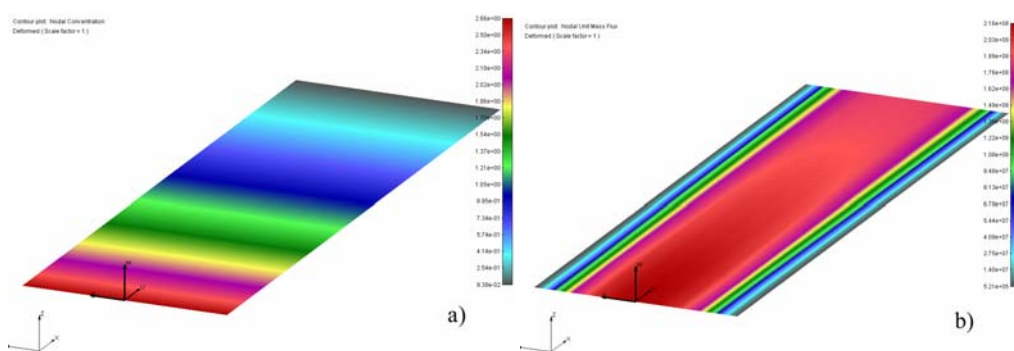
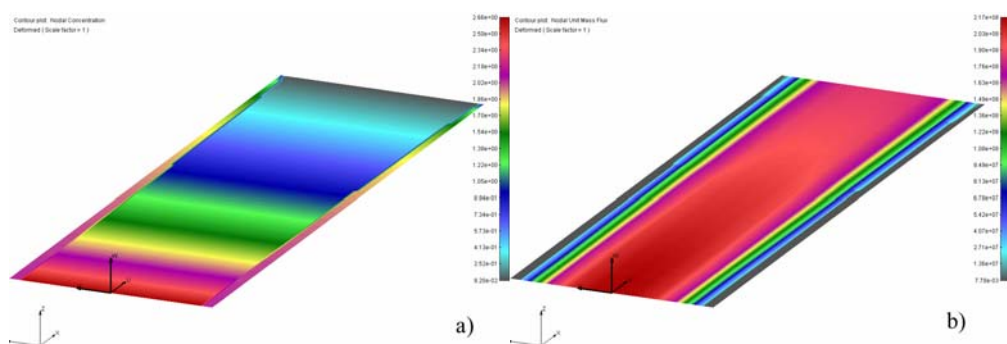**Fig. 5.** Cilindrical model of nanochannel without adsorption effects: a) Field of concentration (units Mol/g) at time t = 0.00003 [h]; b) Field of Unit Mass Flux (units are fg/($\mu^2 \cdot h$)) at time t= 0.00003 [h].

Fig. 6. Cilindrical model of nanochannel with adsorption effects: a) Field of concentration (units Mol/g) at time t = 0.00003 [h]; b) Field of Unit Mass Flux (units are fg/($\mu^2 \cdot h$)) at time t = 0.00003 [h].
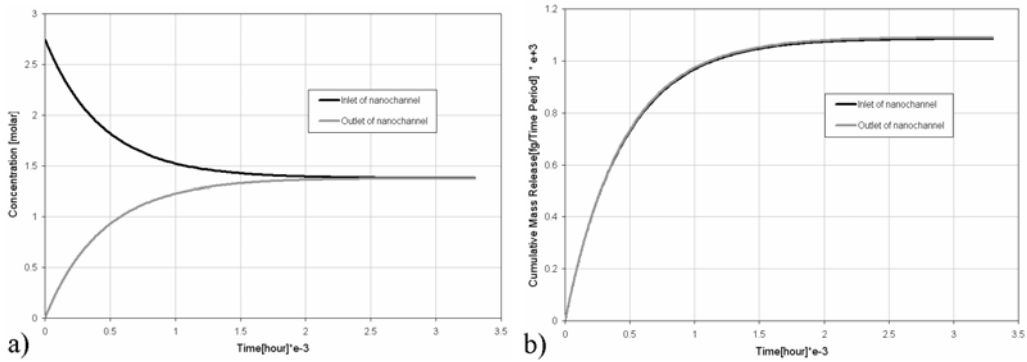
Fig. 7. Cilindrical model of nanochannel with adsorption effects: a) Diagram of concentration change at inlet and outlet cross-section of nanochannel; b) Diagram of Cumulative Mass Release vs time at inlet and outlet cross-sections.
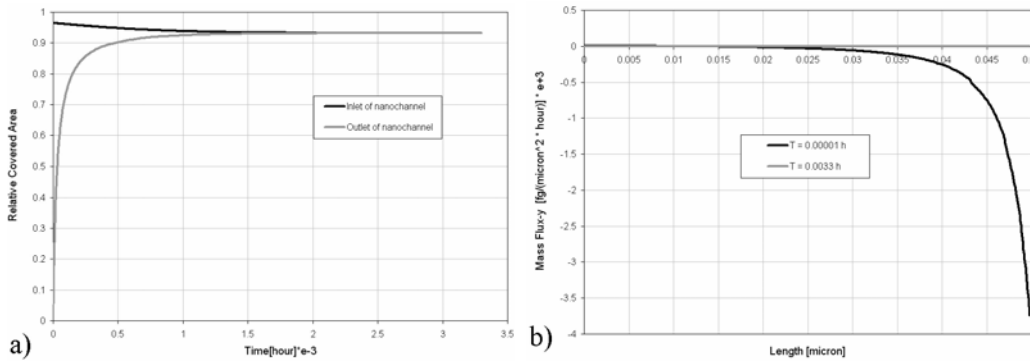

Fig. 8. Cilindrical model of nanochannel with adsorption effects: a) Diagram of Relative Covered Area vs. time at inlet and outlet cross-section of nanochannel; b) Diagram of adsorbed Unit Mass Flux-Y at confined surface for two different time points: t = 0.0001 [h] and at final time t = 0.0033 [h].
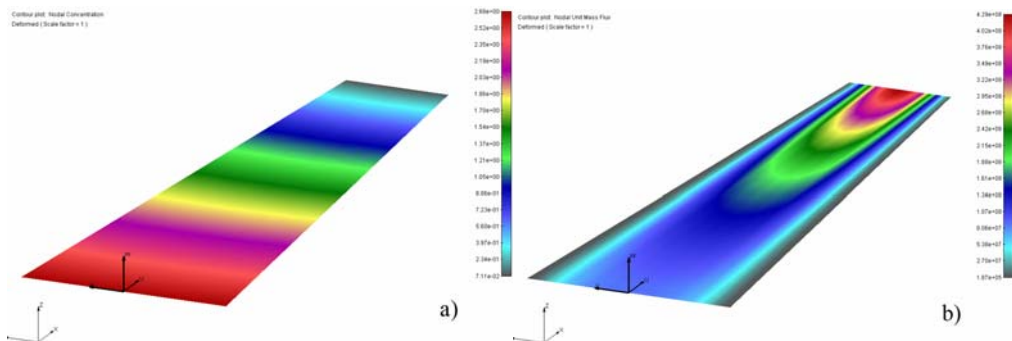
Fig. 9. Conical model of nanochannel with larger inled cross-section and without adsorption effects; a) Field of concentration (units Mol/g) at time t = 0.00006 [h]; b) Field of Unit Mass Flux (units are fg/($\mu^2 \cdot h$)) at t = 0.00006 [h].
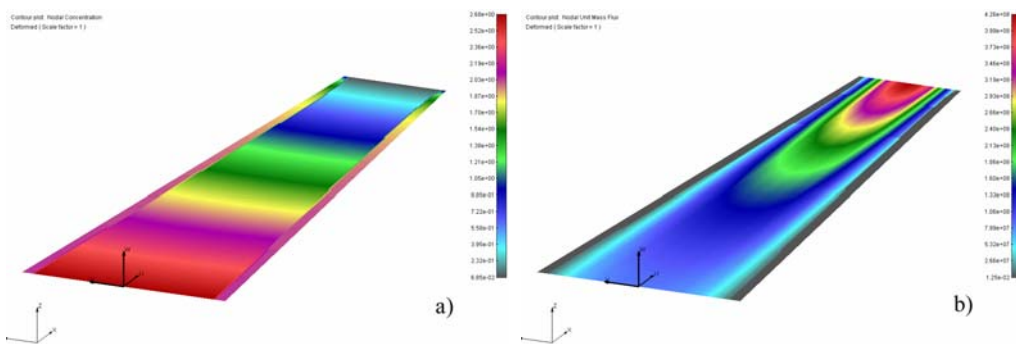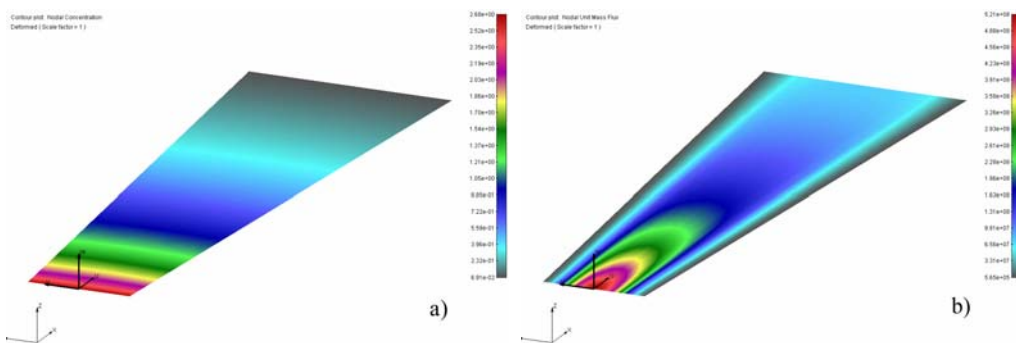

Fig. 10. Conical model of nanochannel with shrink at outlet cross-section and with adsorption effects: a) Field of concentration (units Mol/g) at time t = 0.00006 [h]; b) Field of Unit Mass Flux (units are fg/($\mu^2 \cdot h$)) at t = 0.00006 [h].
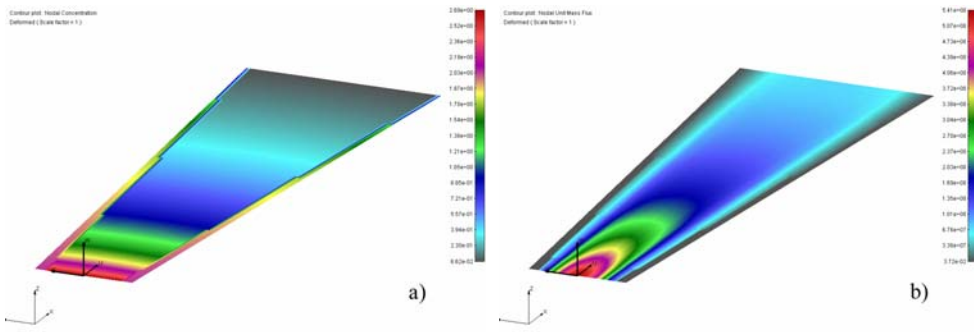

Fig. 11. Conical model of nanochannel with smaller inlet cross-section and without adsorption effects: a) Field of concentration (units Mol/g) at time t = 0.00006 [h]; b) Field of Unit Mass Flux (units are fg/($\mu^2 \cdot h$)) at t = 0.00006 [h].

Fig. 12. Conical model of nanochannel with smaller inlet cross-section and with adsorption effects: a) Field of concentration (units Mol/g) at time t = 0.00006 [h]; b) Field of Unit Mass Flux (units are fg/($\mu^2 \cdot h$)) at t = 0.00006 [h].
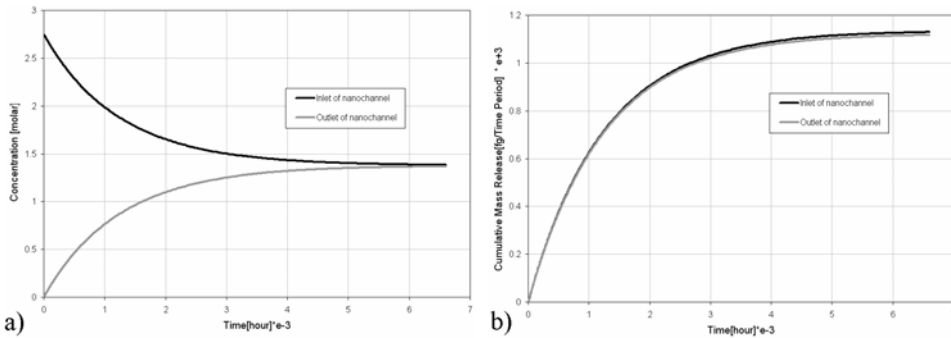

Fig. 13. Conical model of nanochannel with smaller inlet cross-section and with adsorption effects: a) Diagram of concentration change at inlet and outlet cross-section of nanochannel, b) Diagram of Cumulative Mass Release change at inlet and outlet cross-section of nanochannel.
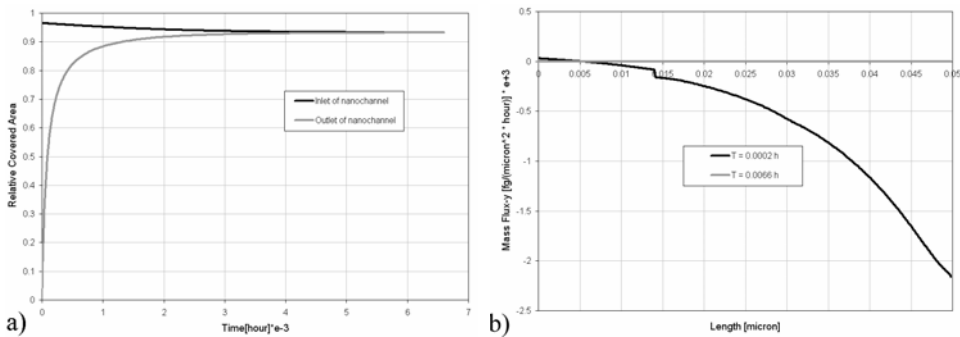

Fig. 14. Conical model of nanochannel with smaller inlet cross-section and with adsorption effects: a) Diagram of Relative Covered Area change at inlet and outlet cross-section of nanochannel, b) Diagram of adsorbed Unit Mass Flux-Y at confined surface for two different time points: t = 0.0002 [h] and at final time t = 0.0066 [h].

3.2. Comments of results

As we discussed before Figs 7.a and 13.a show that concentrations in both reservoirs at the end of FE simulation are the same, which demonstrates accuracy of our numerical procedure and implementation into our software PAK. Also, mass which leaves the inlet reservoir has to be the same with mass which enters the outlet reservoir; this can be seen form Figs 7.b and 13.b). If adsorption effects are includes, it can be seen from Figs 6.a, 10.a and 12.a that concentrations are larger at the interface of nanochannel; they are calculated according to eq. (13). In this zone Mass Flux in longitudal direction is equal to zero (Figs 6.b, 10.b and 12.b), while mass flux in direction normal to the surface is calculated from eq. (17). Relative covered area depends on concentration (eq. 13), which can be seen from diagrams on Figs 8.a and 14.a.

4. Concluding remarks

Based on the hierarchical model for diffusion (Ziemys et al. 2011), which couples MD and macroscale FE methods, we have presented an extension of the model to include adsorption at the surfaces bounding the nano-scale diffusion domain.

Also, a concept of generalization of the model to diffusion through porous media is outlined. This generalized model can lead to development of multiscale models applicable to diffusion in biological environment, as it is in intracellular space, or polymers. Development of these models will certainly require solution of many challenging tasks.

Извод

О дифузији у нанопростору

M. Kojic[1,2], M. Milosevic[1], N. Kojic[3], M. Ferrari[2], A. Ziemys[2]

[1]Metropolitan University – Belgrade, R & D Center for Bioengineering, 34000 Kragujevac, Serbia;
[2]The Methodist Hospital Research Institute, Houston, TX 77030;
[3]Tuftts University, Medford, MA 02155

Резиме

Дифузија у нанопростору се не одвија стриктно по Фиковом закону, који представља основни закон дифузије у макро-окружењима. Одступање од Фиковог закона се јавља због утицаја површина, тј. због интеракције транспортних молекула и граничних површина. Приступ хијерархијског моделирања који узима у обзир утицај граничних површина је представљен у раду Зиемус ет ал. (2011). У хијерархијском моделу се применом концепта молекуларне динамике (МД) врши израчунавање функција скалирања у циљу кориговања дифузионог коефицијента у односу на такозвану "булк" вредност (вредност која одговара слободној дифузији). Затим се, уз коришћење коригованих вредости дифузионог коефицијента, врши моделирање процеса дифузије применом методе коначних елемената (МКЕ) у оквиру инкрементално-итеративне шеме.

У овом раду смо сумирали резултате хијерархијског модела (модела на више скала) и изложили његово уопштење које узима у обзир адсорбцију на зидовима модела. Такође смо дали кратак преглед о могућим даљим применама хијерархијског моделирања процеса дифузије кроз комплексан медијум састављен од дистрибуираних солида, као што је случај са полимерима и биолошким флуидима.

Кључне речи: дифузија, транспорт молекула, молекуларна динамика, метод коначних елемената, утицај површина у нанопросторима.

References

Aggarwal, N., J. Sood, and K. Tankeshwar, Anisotropic diffusion of a fluid confined to different geometries at the nanoscale. Nanotechnology, 2007. 18(33): p. 5.

Alpert, S. and G. Banks, The concentration dependence of the hemoglobin mutual diffusion coefficient. Biophysical Chemistry, 1976. 4(3): p. 287-296.

Bathe, K., Finite element procedures. 1996, Englewood Cliffs, New Jersey: Prentice-Hall.

Broughton, J., et al., Concurrent coupling of length scales: Methodology and application. Physical Review B, 1999. 60(4): p. 2391-2403.

Caro, J., et al., Zeolite membranes-state of their development and perspective. Microporous and Mesoporous Materials, 2000. 38(1): p. 3-24.

Cruz-Chu, E.R., A. Aksimentiev, and K. Schulten, Water-silica force field for simulating nanodevices. J Phys Chem B, 2006. 110(43): p. 21497--21508.

English, A. and M. Dole, Diffusion of sucrose in supersaturated solutions. Journal of the American Chemical Society, 1950. 72(7): p. 3261-3267.

Fine, D., et al., A robust nanofluidic membrane with tunable zero-order release for implantable dose specific drug delivery. Lab on a Chip, 2010.

Gardeniers, H. and A. Berg, Micro-and nanofluidic devices for environmental and biomedical applications. International Journal of Environmental Analytical Chemistry, 2004. 84(11): p. 809-819.

Gladden, J.K. and M. Dole, Diffusion in supersaturated solution-II: glucose solutions. J. Am. Chem. Soc., 1953. 75: p. 3900-3904.

Grattoni, A., et al., Nanochannel Systems for Personalized Therapy and Laboratory Diagnostics. Current Pharmaceutical Biotechnology, 2010. 11(4): p. 343-365.

Hou, T. and X. Wu, A Multiscale Finite Element Method for Elliptic Problems in Composite Materials and Porous Media* 1. Journal of Computational Physics, 1997. 134(1): p. 169-189.

Hughes, T., The finite element method: linear static and dynamic finite element analysis. 2000, New York: Dover Publications.

Iijima, S., Helical microtubules of graphitic carbon. Nature, 1991. 354(6348): p. 56-58.

Jorgensen, W.L., et al., Comparison of simple potential functions for simulating liquid water. Journal of Chemical Physics, 1983. 79(2): p. 926-935.

Karniadakis, G., A. Beskok, and N.R. Aluru, Microflows and nanoflows : fundamentals and simulation. 2005, New York, NY: Springer.

Kojic M, Filipovic N, Tsuda A (2006). A multiscale method for bridging dissipative particle dynamics and Navier-Stokes finite element equations for incompressible fluid and its application in biomechanics. Proc. First South-East European Conference on Comp. Mechanics (Eds. M. Kojic and M. Papadrakakis), Kragujevac, Serbia.

Kojic M, Filipovic N, Stojanovic B, Kojic N (2008a). Computer Modeling in Bioengineering: Theoretical background, examples and software. 200, 8: John Wiley & Sons.

Kojic M, Filipovic N, Tsuda A (2008b). A mesoscopic bridging scale method for fluids and coupling dissipative particle dynamics with continuum finite element method, Comp. Meth. Appl. Mech. Engrg., 197, 821-833.

Kojic, N., A. Kojic, and M. Kojic, Numerical determination of the solvent diffusion coefficient in a concentrated polymer solution. Communications in Numerical Methods in Engineering, 2006. 22(9): p. 1003-1013

Kojic M, Slavkovic R, Grujovic N, Zivkovic M, Filipovic N. (1998, 2009) PAK – FE program for linear and nonlinear analysis for solids, fluids, mass and heat transfer, biomechanics and coupled problems; Mech. Eng. Faculty, University of Kragujevac; R & Center for Bioengineering, Kragujevac, Serbia.

MacKerell Jr, A., et al., All-Atom Empirical Potential for Molecular Modeling and Dynamics Studies of Proteins†. Journal of Physical Chemistry B, 1998. 102(18): p. 3586-3616.

Phillips, J.C., et al., Scalable molecular dynamics with NAMD. J Comput Chem, 2005. 26(16): p. 1781-1802.

Rapaport DC (2004). The Art of Molecular Dynamics Simulation, Cambridge University Press

Rudd, R. and J. Broughton, Coarse-grained molecular dynamics and the atomic limit of finite elements. Physical Review B, 1998. 58(10): p. 5893-5896.

Ziemys, A., et al., Confinement Effects on Monosaccharide Transport in Nanochannels. The Journal of Physical Chemistry B, 2010: p. 132-137.

Ziemys, A., M. Ferrari, and C.N. Cavasotto, Molecular Modeling of Glucose Diffusivity in Silica Nanochannels. Journal of Nanoscience and Nanotechnology, 2009. 9: p. 6349-6359.

Ziemys A, Kojic M, Milosevic M, Kojic N, Hussain F, Ferrari M, Grattoni A (2011). Hierarchical modeling of diffusive transport through nanochannels by coupling molecular dynamics with finite element method, Journal of Computational Physics, 230, 5722–5731.

Wagner GJ, Liu WK (2003). Coupling of atomistic and continuum simulations using a bridging scale decomposition, J. Comput. Phys., 190, 249-274